

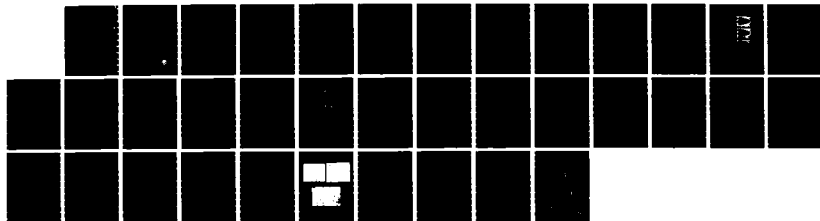
AD-A169 176

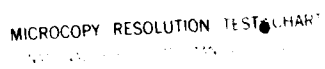
APPLICATION OF NEW TECHNOLOGIES TO RADIATION  
BIODOSIMETRY IN MAMMALIAN SY. (U) ROCHESTER UNIV NY  
SCHOOL OF MEDICINE AND DENTISTRY R M SUTHERLAND ET AL.  
FEB 86 USAFSAM-TR-85-66 F33615-84-C-8603 F/G 6/18

1/1

UNCLASSIFIED

NL





MICROCOPY RESOLUTION TEST CHART

USAFSAM-TR-85-66

# APPLICATION OF NEW TECHNOLOGIES TO RADIATION BIODOSIMETRY IN MAMMALIAN SYSTEMS

Robert M. Sutherland, Ph.D.  
Edith M. Lord, Ph.D.  
Peter C. Keng, Ph.D.

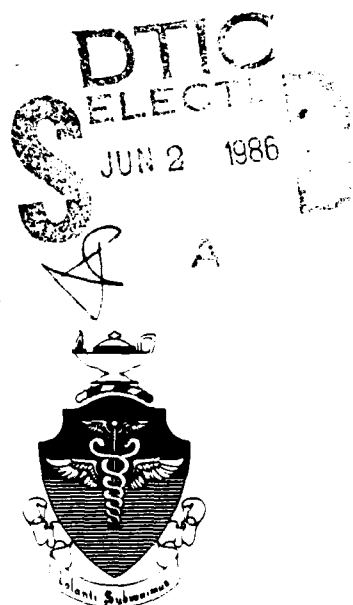
University of Rochester  
School of Medicine and Dentistry  
Cancer Center, Box 704  
601 Elmwood Avenue  
Rochester, New York 14642

February 1986

Final Report for Period January 1984 -- December 1984

Approved for public release; distribution is unlimited.

Prepared for  
USAF SCHOOL OF AEROSPACE MEDICINE  
Aerospace Medical Division (AFSC)  
Brooks Air Force Base, TX 78235-5301



FILE COPY

## NOTICES

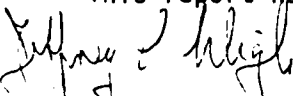
This final report was submitted by the School of Medicine and Dentistry, University of Rochester, Rochester, New York 14642, under contract F33615-84-C-0603, job order 7757-04-37, with the USAF School of Aerospace Medicine, Aerospace Medical Division, AFSC, Brooks Air Force Base, Texas. Captain Jeffrey C. Wigle (USAFSAM/RZB) was the Laboratory Project Scientist-in-Charge.

When Government drawings, specifications, or other data are used for any purpose other than in connection with a definitely Government-related procurement, the United States Government incurs no responsibility nor any obligation whatsoever. The fact that the Government may have formulated or in any way supplied the said drawings, specifications, or other data, is not to be regarded by implication, or otherwise in any manner construed, as licensing the holder, or any other person or corporation; or as conveying any rights or permission to manufacture, use, or sell any patented invention that may in any way be related thereto.

The animals involved in this study were procured, maintained, and used in accordance with the Animal Welfare Act and the "Guide for the Care and Use of Laboratory Animals" prepared by the Institute of Laboratory Animal Resources - National Research Council.

The Office of Public Affairs has reviewed this report, and it is releasable to the National Technical Information Service, where it will be available to the general public, including foreign nationals.

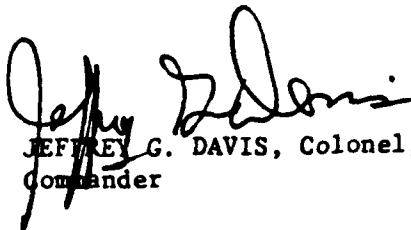
This report has been reviewed and is approved for publication.



JEFFREY C. WIGLE, Captain, USAF, BSC  
Project Scientist



DAVID H. WOOD, Lt Col, USAF, BSC  
Supervisor



JEFFREY G. DAVIS, Colonel, USAF, MC  
Commander

UNCLASSIFIED

SECURITY CLASSIFICATION OF THIS PAGE

## REPORT DOCUMENTATION PAGE

|   |       |  |  |  |                                   |
|---|-------|--|--|--|-----------------------------------|
| 1a. REPORT SECURITY CLASSIFICATION<br><b>UNCLASSIFIED</b>   |       |  | 1b. RESTRICTIVE MARKINGS   |  |                                   |
| 2a. SECURITY CLASSIFICATION AUTHORITY   |       |  | 3. DISTRIBUTION/AVAILABILITY OF REPORT<br>Approved for public release; distribution is unlimited.                      |  |                                   |
| 2b. DECLASSIFICATION/DOWNGRADING SCHEDULE   |       |  | 4. PERFORMING ORGANIZATION REPORT NUMBER(S)  |  |                                   |
| 4. PERFORMING ORGANIZATION REPORT NUMBER(S)   |       |  | 5. MONITORING ORGANIZATION REPORT NUMBER(S)<br><br>USAFSAM-TR-85-66  |  |                                   |
| 6a. NAME OF PERFORMING ORGANIZATION<br>University of Rochester<br>School of Med. & Dentistry  |       | 6b. OFFICE SYMBOL<br>(If applicable)         |  | 7a. NAME OF MONITORING ORGANIZATION<br>USAF School of Aerospace Medicine (RZB) |                                   |
| 6c. ADDRESS (City, State and ZIP Code)<br>Cancer Center, Box 704<br>601 Elmwood Avenue<br>Rochester, New York 14642   |       |  | 7b. ADDRESS (City, State and ZIP Code)<br>Aerospace Medical Division (AFSC)<br>Brooks Air Force Base, Texas 78235-5301 |  |                                   |
| 8a. NAME OF FUNDING/SPONSORING ORGANIZATION   |       | 8b. OFFICE SYMBOL<br>(If applicable)         |  | 9. PROCUREMENT INSTRUMENT IDENTIFICATION NUMBER<br>F33615-84-C-0603            |                                   |
| 8c. ADDRESS (City, State and ZIP Code)  |       |  | 10. SOURCE OF FUNDING NOS.   |  |                                   |
|   |       |  | PROGRAM<br>ELEMENT NO.<br>62202F   | PROJECT<br>NO.<br>7757   | TASK<br>NO.<br>04                 |
|   |       |  | WORK UNIT<br>NO.<br>37   |  |                                   |
| 11. TITLE (Include Security Classification)<br>APPLICATION OF NEW TECHNOLOGIES TO RADIATION BIODOSIMETRY IN MAMMALIAN SYSTEMS   |       |  |  |  |                                   |
| 12. PERSONAL AUTHOR(S)<br>Sutherland, Robert M.; Lord, Edith M.; and Keng, Peter C.   |       |  |  |  |                                   |
| 13a. TYPE OF REPORT<br>Final Report   |       | 13b. TIME COVERED<br>FROM 31Jan84 TO 31Dec84 |  | 14. DATE OF REPORT (Yr., Mo., Day)<br>1986, February                           |                                   |
|   |       |  |  | 15. PAGE COUNT<br>36   |                                   |
| 16. SUPPLEMENTARY NOTATION  |       |  |  |  |                                   |
| 17. COSATI CODES  |       |  | 18. SUBJECT TERMS (Continue on reverse if necessary and identify by block number)                                      |  |                                   |
| FIELD   | GROUP | SUB. GR.                                     | Radiation biodosimetry, Centrifugal elutriation, Flow cytometry, Alkaline elution, Premature chromosome condensation   |  |                                   |
| 06  | 18    |  |  |  |                                   |
| 06  | 03    |  |  |  |                                   |
| 19. ABSTRACT (Continue on reverse if necessary and identify by block number)<br>Mononuclear cells from peripheral blood are presently the best candidates for a space radiation biodosimeter for man because they are easily obtained, and are among the most radiosensitive cells in the body. They are, however, members of a highly heterogeneous population of cell subtypes potentially differing in radiosensitivities. To study the cell subpopulation holding the greatest potential for use as a biodosimeter, the cell types must be uniquely identified and/or separated so that subtle effects on radiosensitive cells are not masked by "non-effects" on relatively radioresistant cells present in a mixed population.<br><br>Flow cytometry and centrifugal elutriation are proving to be useful for identifying and separating individual subpopulations from heterogeneous mixtures of cells. Flow cytometry uses fluorescent antibodies to label and sort the cells of interest, while centrifugal elutriation utilizes counterbalanced centrifugal and fluid flow forces |       |  |  |  |                                   |
| 20. DISTRIBUTION/AVAILABILITY OF ABSTRACT<br>UNCLASSIFIED/UNLIMITED <input checked="" type="checkbox"/> SAME AS RPT. <input type="checkbox"/> DTIC USERS <input type="checkbox"/>   |       |  | 21. ABSTRACT SECURITY CLASSIFICATION<br>UNCLASSIFIED   |  |                                   |
| 22a. NAME OF RESPONSIBLE INDIVIDUAL<br>Jeffrey C. Wigle, Capt, USAF, BSC  |       |  | 22b. TELEPHONE NUMBER<br>(Include Area Code)<br>(512) 536-3416   |  | 22c. OFFICE SYMBOL<br>USAFSAM/RZB |

DD FORM 1473, 83 APR

EDITION OF JAN 73 IS OBSOLETE.

UNCLASSIFIED

SECURITY CLASSIFICATION OF THIS PAGE

## 19. ABSTRACT (continued)

to separate cells by size. In combination with two analytical procedures (premature chromosome condensation (PCC) and alkaline elution), these two techniques have been applied to study radiation effects on mononuclear cells from mouse peripheral blood irradiated *in vivo*, and cell cycle phase specific repair of single-strand breaks in cellular deoxyribonucleic acid (DNA) of the Chinese hamster ovary (CHO) fibroblast cell line irradiated *in vitro*.

Whole-body irradiation of mice produced significant decreases in total white blood cell count following as little as 100 rads. The strongest response was in the lymphocyte compartment, B-lymphocytes were the most sensitive, as measured by binding of antibody to surface immunoglobulin (Ig), and the maximum effect is found about 4 days postirradiation. Functional capacity of T- and B-lymphocytes was also determined following irradiation *in vivo* by measuring the ability of the cells to proliferate in response to the mitogens Con A and lipopolysaccharide, respectively. T- and B-lymphocytes both showed altered functional capacity following a dose of 100 rads, with maximum effect occurring at 3 days postirradiation and a return to normal 5 days postirradiation.

Radiation-induced DNA and chromosome damage in CHO fibroblasts was also studied. Using alkaline elution, radiation damage from doses of as little as 25-50 rads could be detected in asynchronously growing cells, and a quantitative relationship between elution rate and radiation dose was established. Alkaline elution was also used to measure induction and repair of single strand breaks in DNA of cells synchronized in G<sub>1</sub>, S, and G<sub>2</sub>+M phases by centrifugal elutriation. No significant difference in break formation was found as a function of cell cycle phase, but G<sub>2</sub>+M phase cells had a significantly slower repair rate than G<sub>1</sub> and S phase cells, which were the same. Premature chromosome condensation analysis demonstrated a direct relationship between radiation dose and chromosome damage in the dose range of 0-500 rads, and the detection of damage after as little as 50 rads.

## TABLES OF CONTENTS

|   | <u>Page</u> |
|---|-------------|
| INTRODUCTION.....   | 1           |
| Statement of the Problem.....                                 | 1           |
| Experimental Approach to the Problem.....                     | 1           |
| METHODS AND PROCEDURES.....                                   | 3           |
| Centrifugal Elutriation.....                                  | 3           |
| Principles and Instruments.....                               | 3           |
| Procedures.....   | 5           |
| Flow Cytometry.....   | 6           |
| Principles and Instruments.....                               | 6           |
| Cell Cycle Analysis Procedures.....                           | 8           |
| Alkaline Elution.....   | 8           |
| Principles and Instruments.....                               | 8           |
| Procedures.....   | 9           |
| Premature Chromosome Condensation.....                        | 10          |
| Principles.....   | 10          |
| Procedures.....   | 10          |
| Analysis of Radiation Effects on Peripheral Blood Cells.....  | 11          |
| Immunofluorescence: Cell Preparation.....                     | 11          |
| Immunofluorescence Staining.....                              | 12          |
| Assays of Lymphocyte Function: Mitogenic Response Assays..... | 12          |
| Irradiation.....  | 13          |
| Animals.....  | 13          |
| RESULTS.....  | 13          |
| DISCUSSION.....   | 27          |
| REFERENCES.....   | 28          |

## FIGURES

Fig.  
No.

1. The diagram of elutriation separation chamber and the principles of physical parameters governing the separation properties.....4
2. Schematic diagram of the Beckman JE-6 elutriator system.....6
3. Schematic diagram of a Coulter EPIC V flow cytometer/cell sorter.....7
4. Schematic diagram of the alkaline elution system.....9
5. Premature chromosome condensation obtained from a PEG fused CHO mitotic and interphase cell.....11
6. Flowchart of experimental procedures for analysis of radiation effects on peripheral blood lymphocytes.....12

|     |  |    |
|-----|--|----|
| 7.  | Kinetics of the radiation dose response of the number of white blood cells/ml of blood present after 0-rad ( ), 100-rad ( ), or 400-rad ( ) whole-body irradiation.....  | 15 |
| 8.  | Two-dimensional flow cytometry histogram showing the autofluorescence of unstained peripheral blood lymphocytes from control mice and irradiated (400 rads) mice 7 days post irradiation.....  | 15 |
| 9.  | Two-dimensional flow cytometry histogram showing the differences in intensity of H-20 <sup>d</sup> surface fluorescence staining of control cells (H-2C) and PBL from mice receiving 400-rad whole-body irradiation 7 days previously..... | 16 |
| 10. | Two-dimensional flow cytometry histogram showing a marked decrease in cells positive for the T-cell marker Thy-1 in mice receiving 400-rad irradiation (Thy-1 Irr) as compared to control mice (Thy-1 C).....                              | 17 |
| 11. | Two-dimensional flow cytometry histogram showing the virtual elimination of surface Ig <sup>+</sup> cells (B-lymphocytes) of the PBL from mice receiving 400-rad irradiation.....  | 17 |
| 12. | Cell volume distribution of unseparated (A) and elutriated (B) CHO cells measured by Coulter channelyzer.....  | 21 |
| 13. | DNA histograms of asynchronous CHO cells (A) and separated G <sub>1</sub> , S, and G <sub>2</sub> +M cells (B).....  | 21 |
| 14. | Alkaline elution profiles of CHO cells irradiated with 0-800-rad Cs-137 gamma rays.....  | 22 |
| 15. | Alkaline elution profiles of CHO cells irradiated with a single dose of 1000 rads and incubated at 37° C for 30 min, 45 min, 1 h, 2 h, 4 h, and 6 h.....   | 22 |
| 16. | Formation of DNA single-strand breaks at G <sub>1</sub> , S, and G <sub>2</sub> +M phases of the cell cycle in CHO cells.....  | 23 |
| 17. | Repair kinetics of DNA single-strand breaks at G <sub>1</sub> , S, and G <sub>2</sub> +M phases of the cell cycle after 1000-rad Cs-137 gamma rays.....  | 23 |
| 18. | Repair kinetics of DNA cross-links in G <sub>1</sub> , S, and G <sub>2</sub> +M CHO cells following 5-krad gamma rays.....   | 24 |
| 19. | Premature chromosome condensation of CHO cells irradiated with 100-rad (A), 300-rad (B), and 500-rad (C) Cs-137 gamma rays.....  | 25 |
| 20. | Relationship of radiation dose and chromosome aberrations in CHO cells irradiated with 0-500-rad Cs-137 gamma rays.....  | 26 |



## Tables

| <u>Table<br/>No.</u>  | <u>Page</u> |
|---|-------------|
| 1. Differential cell counts on peripheral blood subpopulations<br>following irradiation.....      | 14          |
| 2. Flow cytometric analysis of the effect of radiation on<br>peripheral blood subpopulations..... | 18          |
| 3. Effect of radiation on the function of peripheral blood lymphocytes...                         | 19          |

100-100-100

☒ WTIS C&AI  
☐ DTIC TAB  
☐ Unannounced  
 Justification

By \_\_\_\_\_

Distribution/

Availability Codes

Dist Avail and/or Special

A-1



# APPLICATION OF NEW TECHNOLOGIES TO RADIATION BIODOSIMETRY IN MAMMALIAN SYSTEMS

## INTRODUCTION

### Statement of the Problem

Spacecrews face the potential hazard of exposure to solar and other ionizing radiation of a range of qualities and energies. Exposures to this radiation are measured by appropriate physical dosimeters placed on the crewmembers and at different locations on the spacecraft. However, for a variety of reasons these dosimeters probably will not accurately reflect the "biologically experienced" dose of the individual crewmembers. The mixture of radiation may vary in time relative to solar flare events and location of space orbits. Also, partial body exposures of different doses would be expected due to differences in shielding within the spacecraft or during extravehicular maneuvers by the crew in flight or at space stations. The relative biological effectiveness (RBE) would be very difficult to estimate under these conditions from physical dosimetry measurements. In-flight and relatively current information on acute and chronic biological damage expected from these radiation exposures is critically important for decisions regarding possible termination of flights and deployment of crew for in-flight tasks during long missions or for future assignments. Therefore, the development of appropriate accurate biodosimetry methodology is of extreme importance.

Most useful would be methodology which imposed minimal discomfort or inconvenience to the personnel being monitored and allowed assessment at regular intervals, perhaps weekly, to determine the biological significance of the doses received. A potentially excellent source of biological material for analysis is the hemopoietic cells of the immune system since the radiation sensitivity of these cells, particularly the lymphocyte population, is well documented and these cells are easily obtained from small samples of peripheral blood. However, the sensitivity and thus usefulness of such analysis requires the development of instrumentation and technologies to permit detection of small alterations which may result from exposure to low radiation levels and which may occur only in subpopulations of such cells.

### Experimental Approach to the Problem

The most previous radiation studies on these cells (1) were performed prior to the realization that this is a highly heterogeneous population composed of several cell subtypes which may have markedly different radiation sensitivities. The methodologies which are available to us and described here would allow us to analyze these individual subpopulations and determine the inherent sensitivities of each. Since many of these cells and the factors they produce, play a major role in the regulation of the immune response, radiation-induced alterations in their proportions or numbers may have marked effects on the health status of exposed individuals.

Two technologies, centrifugal elutriation (2,3) and flow cytometry (4,5,6), are proving to be especially useful for identifying and separating individual subpopulations from highly heterogeneous mixtures of cells. In the centrifugal elutriation technique, two forces, the centrifugal force sedimenting cells and a force associated with fluid flowing in the opposite direction, are counterbalanced such that the cells in the chamber segregate and relatively homogeneous populations based on size and density can be obtained. Thus cells with relatively small differences, such as different types of peripheral blood leucocytes or different cell growth cycle stages of cells, can be separated.

Flow cytometry is another highly useful technique which can identify and separate cells on the basis of many biological properties using fluorescent chemical markers and size. The cells are confined to the center of a liquid stream and pass one at a time through a laser beam. The resulting signals are electronically processed and stored, determining whether or not each individual cell meets certain preselected criteria. Several different parameters including deoxyribonucleic acid (DNA) content, ribonucleic acid (RNA) content, surface antigens, as well as physical properties such as size, shape, and refractive index can be measured simultaneously on individual cells. The advantages of this instrumentation over conventional microscopic analysis are several. Large numbers of cells can be analyzed in shorter periods of time (2000/s) and quantitative rather than simply qualitative determinations can be made. In addition, cells meeting a given set of predetermined criteria can be physically sorted from the remaining cells.

The flow cytometer located within our laboratories is a Coulter Electronics EPICS V dual laser instrument outfitted with a Multiparameter Data Acquisition and Display System (MDADS), a microprocessor with six analog-to-digital convertors permitting the analysis and sorting on six separate signals. This instrument, which is the most advanced design available commercially is physically located directly adjacent to the centrifugal elutriation laboratory.

Another recent scientific advance, the development of hybridoma technology for the production of monoclonal antibodies (7), has further increased the analytical capabilities of flow cytometry by providing well-defined consistent reagents for identifying cells by virtue of cell surface markers detectable with fluorescent antibodies (8). Our laboratory has been actively producing such reagents and also has available a wide variety of other antibodies produced by colleagues.

The alkaline elution technique has been used recently to measure DNA damage (strand breaks, DNA-protein cross-links and DNA-DNA cross-links) and the repair of different types of DNA lesions (9). This technique is able to measure the DNA damage and repair in the radiobiologically relevant dose range (0-1000 rads). We have also developed a fluorescent method to measure the DNA content after this alkaline elution procedure so that this technique can be applied to an in vivo sample such as lymphocytes.

Damage to genetic material induced by radiation can also be visualized and measured at the chromosome level. Breaks in chromosomes are normally scored at the time of cell division when the chromosomes are in a condensed form. The utility of this technique has been greatly increased by a new method which involves induction of cells to condense the chromatin material at phases of the cell cycle prior to cell division. This technique makes it possible to evaluate cells which may not normally divide and at sensitive phases of the cell cycle before any repair occurs. This premature chromosome condensation (PCC) method involves fusion of a dividing nonirradiated cell with an irradiated cell to form a hybrid (10,11).

By combining several technologies to study irradiated cells, both lymphocytes as well as in vitro cell lines as models for other tissue cells, it is possible to determine relative radiosensitivities of cell subpopulations in terms of several parameters. These parameters include the changes in numbers of different cell subpopulations, functional alterations, cell survival, and DNA/chromosome lesions and their repair.

Clearly, considerable developmental work is required to establish such systems for radiation biodosimetry in humans. Therefore, we report here results of studies using cells from experimental animals (mice) and mammalian in vitro cell lines to evaluate these methods. Centrifugal elutriation techniques were developed to separate populations of lymphoid cells (lymphocytes, granulocytes, and monocytes) from peripheral blood of mice and to obtain synchronous populations of G<sub>1</sub>, S, and G<sub>2</sub>+M cells from the Chinese Hamster Ovary (CHO) cell line grown in vitro. Flow cytometric techniques were then optimized using fluorescein conjugated monoclonal antibodies directed toward surface markers, to further analyze these subpopulations of lymphoid cells. Once the use of these techniques was optimized, dose-response curves after in vitro gamma radiation at doses of 0-1000 rads were determined for the CHO cells. Viability of the CHO cells after such treatment was assessed by colony formation assay. The alkaline elution and PCC techniques for assessing DNA/chromosome damage and repair were compared for relative sensitivity. These studies were expanded to develop preliminary in vivo dose responses of individual cell lymphoid subpopulations in the peripheral blood of mice given whole-body irradiation.

## METHODS AND PROCEDURES

### Centrifugal Elutriation

#### Principles and Instruments

Separation of subpopulations of cells by centrifugal elutriation depends on a balance of an outwardly directed centrifugal force and inwardly directed fluid flow and buoyant forces. A suspended cell reaches its equilibrium position in the separation chamber (Fig.1, A and B) according to its sedimentation velocity, which is based on its size, density, and shape. When either the rotor speed (i.e., the centrifugal force) is decreased or the velocity of the fluid flow is increased, successive fractions containing relatively homogeneous-sized (Fig. 1C) populations of cells can be collected.

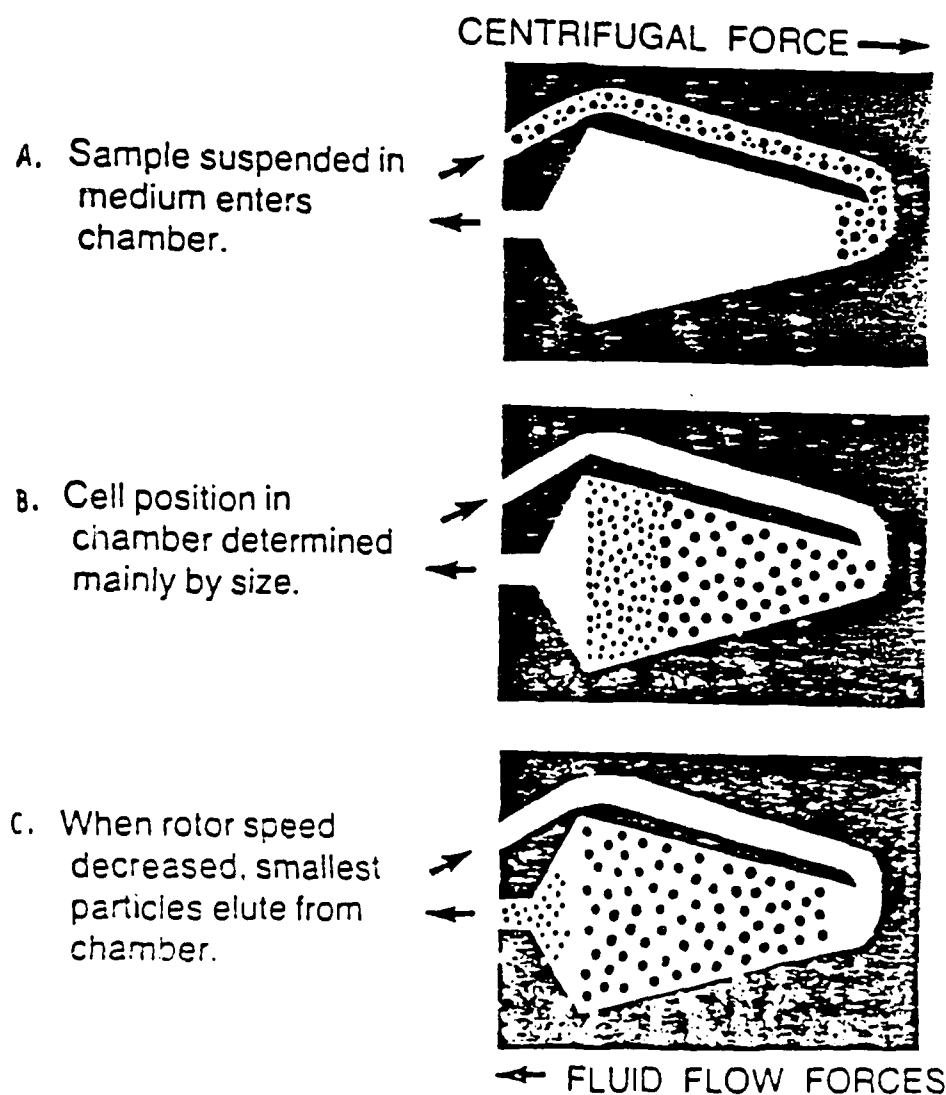


Figure 1. The diagram of elutriation separation chamber and the principles of physical parameters governing the separation properties.

The physical theory of centrifugal elutriation is based on the relationship between the volume ( $V$ ) of the cells and the collection rotor speed ( $\omega$ ) or the fluid flow rate ( $v$ ). The equation for centrifugal elutriation can be established by equilibrating the three forces acting on the spherical particle with diameter ( $d$ ); centrifugal force ( $F_c$ ), buoyant force ( $F_b$ ), and fluid drag force ( $F_d$ )

$$F_c = \left( \frac{\pi}{6} \right) d^3 \rho \omega^2 R \quad (1)$$

$$F_b = - \left( \frac{\pi}{6} \right) d^3 \rho_c \omega^2 R \quad (2)$$

$$F_d = -3\pi \eta d v \quad (3)$$

Where:

$\omega$  = rotor angular velocity  
 $R$  = distance from cell to the center of the rotor  
 $\rho$  = fluid density  
 $\rho_c$  = cell density  
 $\eta$  = fluid viscosity  
 $v$  = local fluid viscosity

When a cell is at equilibrium in the chamber:

$$F_c + F_b + F_d = 0 \quad (4)$$

and the volume of the cells being removed from the separation chamber is:

$$V = k \omega^3 \quad (5)$$

where:

$$k = 9 \pi \sqrt{2} \left[ \eta / (\rho - \rho_c) \right] \frac{3}{2} \quad (6)$$

under constant fluid flow rate conditions.

## Procedures

Centrifugal elutriation procedures have been used in this project to collect homogeneous populations of G<sub>1</sub> (>95%) cells, S (>80%) cells, and G<sub>2</sub>+M (>80%) cells from CHO cell cultures. We have also developed procedures to separate different lymphoid cell populations (i.e., lymphocytes, granulocytes, and macrophages) from murine and human systems using centrifugal elutriation.

The schematic diagram of the elutriator system is shown in Figure 2. Cells were fractionated using the Beckman JE-6 elutriator rotor driven by a modified Beckman J21-C or J2-21 centrifuge. The Sanderson separation chamber was used for all the experiments. The centrifuge speed was controlled by a 10-turn potentiometer to permit rotor speed selection to within  $\pm 10$  revolutions per minute (rpm). Rotor speed was measured directly with stroboscopic counting of the rpm. This strobe light, situated beneath the rotor, allowed visualization of the separation chamber during operation. Fluid flow through the elutriator system was maintained by a Multiperpex pump with fine velocity control. The flow rate was continuously monitored using an in-line flow meter.

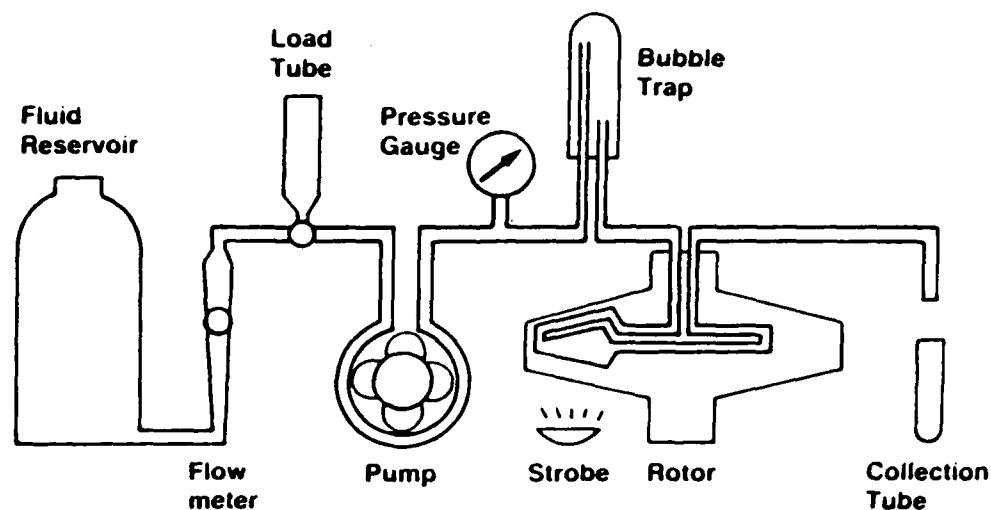


Figure 2. Schematic diagram of the Beckman JE-6 elutriator system.

Chinese hamster ovary (CHO) cells were grown in tissue culture using F-10 medium containing 10% fetal calf serum as previously described. Exponentially growing CHO cells were trypsinized from monolayer cultures and elutriated in ice-cold F-10 medium. During elutriation, the reservoir, rotor, and collection tubes were kept at 4° C. The flow rate during elutriation was kept constant at 35 ml/min. A long collection method was designed to increase the cell yield with a minimum decrease in homogeneity. After loading the cells at 3400 ( $\pm 10$ ) rpm, a total of 200 ml of fluid was collected. Then the rotor speed was decreased in small intervals to 2000 ( $\pm 10$ ) rpm with 2 fractions of 40-ml sample collected. A total of 66 fractions were collected for CHO synchrony experiments. The separated fractions were counted with a Coulter channelyzer system to determine the size distribution of separated cells. Flow cytometry analysis and autoradiography were used to confirm the degree of synchrony of G<sub>1</sub>, S, and G<sub>2</sub>+M cells.

For separating different lymphoid cell populations from mice, cells were loaded into the elutriator system with a flow rate of 12.5 ml/min and a rotor speed of 4040 ( $\pm 10$ ) rpm. A series of 40-ml samples were collected at each rotor speed drop. An approximate relation between the rotor speed and particular types of homogeneous populations of cells collected at that rotor speed is listed below:

|              |               |                          |
|--------------|---------------|--------------------------|
| lymphocytes  | 3550-3250 rpm | 5 - 6 $\mu$ m cell dia   |
| granulocytes | 3000-2700 rpm | 7.5 $\mu$ m cell dia     |
| macrophages  | 2500-2200 rpm | 10 - 12 $\mu$ m cell dia |

### Flow Cytometry

#### Principles and Instruments

The basic principle of flow cytometry was introduced about 25 years ago with the first Coulter counter; electronic measurements were made on

cells flowing one cell at a time past a measurement point. With the advancement in computers and electronics, the current flow cytometry system in our research group has 4 component systems: (1) light sources, argon, and krypton lasers; (2) a sample chamber and optical assembly; (3) a set of associated electronics (photomultiplier tubes) that convert light impulses to digital signals (ADC converters); and (4) a computer system that controls instrument operations, collects data, and performs analytical routines. A diagram of the flow cytometry system is shown in Figure 3.

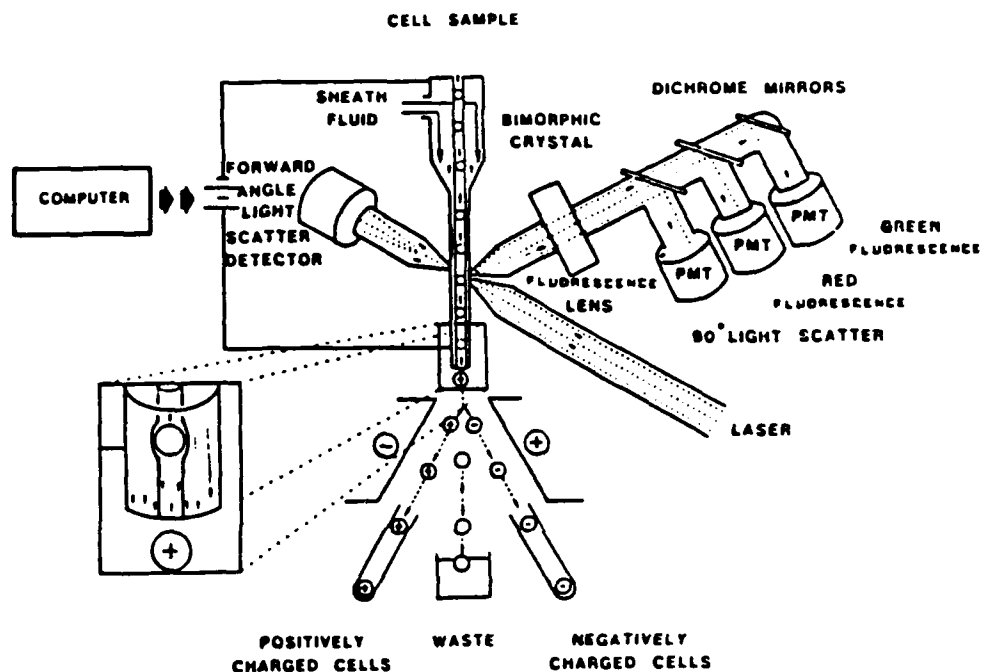


Figure 3. Schematic diagram of a Coulter EPIC V flow cytometer/cell sorter.

During operation an isotonic sheath fluid is forced under pressure into a V-shaped nozzle assembly and exits through a small orifice which is 76  $\mu\text{m}$  in diameter. The exit speed is approximately 10 m/s. The nozzle geometry creates a laminar flow within the nozzle into which a sample insertion tube is positioned. The sample is pressurized at a higher differential pressure than the sheath fluid and is introduced to the nozzle through the sample insertion tube. The sheath flow in the nozzle creates a hydrodynamic focusing effect and draws the sample fluid into the stream and surrounds it with sheath fluid. The cells in the sample fluid then pass through a pinpoint laser light source immediately after exiting the nozzle assembly.

Two major events occur when the cell is intercepted by the laser beams. First, the light from the point source is scattered by the cell. Second, fluorescence occurs when a fluorochrome-containing cell absorbs the laser



light at the incident wavelength and then reemits the light at a lower wavelength. Signals from light scattering (both forward angle and 90° angle) and fluorescence falling upon the detectors are converted by photomultiplier tubes to an electronic impulse which is then processed by an analog-to-digital converter to a digital signal. In most applications this number is recorded and analyzed by the computer system.

In addition to data analysis, the flow cytometer has the capability of cell sorting. When the computer detects that a cell satisfying the sort logic is in the sample stream, an electrical charge is placed upon the stream. As the droplet containing the cell of interest breaks off from the main stream, the stream is discharged. As the droplet moves down stream, it enters an electrical field created by two charged plates: one charged positively and one negatively. The droplet is attracted to the plate with the opposite charge, and is consequently deflected away from the main stream and collected in an appropriate test tube or microplate. Extremely pure populations of cells may be sorted at a relatively rapid rate.

### **Cell Cycle Analysis Procedures**

Mithramycin staining was performed on synchronized cell population. Cells isolated from centrifugal elutriation were fixed with 75% ethanol at a concentration of  $10^6$  cells/3 ml ethanol. The fixed cells were washed twice with phosphate buffered saline (PBS), centrifuged, and resuspended in ice-cold mithramycin solution (0.1 mg mithramycin/ml in PBS + 12.5 mM  $MgCl_2$ ) at a concentration of  $10^6$  cells/ml. The cell suspension was then aspirated 3 times with an 18G needle to break up any cell clumps, and filtered through a 37- $\mu$ m nylon mesh. Flow cytometry analyses were performed in stirred samples at 4 °C, following staining for 60 min, with laser excitation at 457 nm. Deoxyribonucleic acid fluorescence intensity was monitored following a 510-nm laser interference filter and a 515-nm long-pass filter. The percentages of  $G_1$ , S, and  $G_2$ +M cells from the DNA histograms were analyzed using a computer program based on mathematical models developed by Dean and Jett.(9)

### **Alkaline Elution**

#### **Principles and Instruments**

The alkaline elution technique was developed by Kohn and colleagues (10). The technique measures the rate at which single-stranded DNA, released from cells in high alkaline condition, passes through holes in a filter. This rate depends in a quantitative manner on the length of the DNA strands, the number of DNA interstrand, and DNA protein cross-links. Thus, this method can give sensitive and convenient measurements of DNA strand breaks and DNA cross-links. Intact DNA from unirradiated cells passes through the filter very slowly, whereas the introduction of strand breaks speeds up this process; this makes it possible to detect the initial yield of strand breaks after as little as 25 rad. Cross-links in the DNA are detected by the reduced elution rate of DNA due to the increased DNA strand size (interstrand cross-links) or the adsorption of protein to polyvinylchloride (PVC) filters (DNA protein cross-links). Deoxyribonucleic acid interstrand

cross-links are differentiated from DNA protein cross-links by the sensitivity of the latter to proteinase K.

The apparatus and the principle of alkaline elution are shown in Figure 4. The full apparatus in the alkaline elution assay consists of a cylindrical filter holder of 25-mm dia, long enough to hold approximately 50 ml of elution solution. Polycarbonate (PC) or PVC filters, 2  $\mu$ m pore size, 25-mm dia, are used. The elution process is carried out by pumping the elution solution at a slow, constant, and reproducible speed without pulsation, using a Gilson Minipuls II 8-channel pump equipped with a slow speed gearbox. Fractions are collected directly into glass tubes using a LKB 2115 fraction collector. Data are represented on a semilog plot as fraction of DNA retained vs elution time. A linear relationship can be established between the amount of DNA single-strand breaks and radiation dose received. For DNA cross-links, a quantitative measure of cross-link factor (CF) is given:

$$CF = \frac{\log R_0}{\log R} \quad (7)$$

where  $R_0$  and  $R$  are the fraction of DNA retained by control and treated cells respectively, determined at a fixed time of elution.

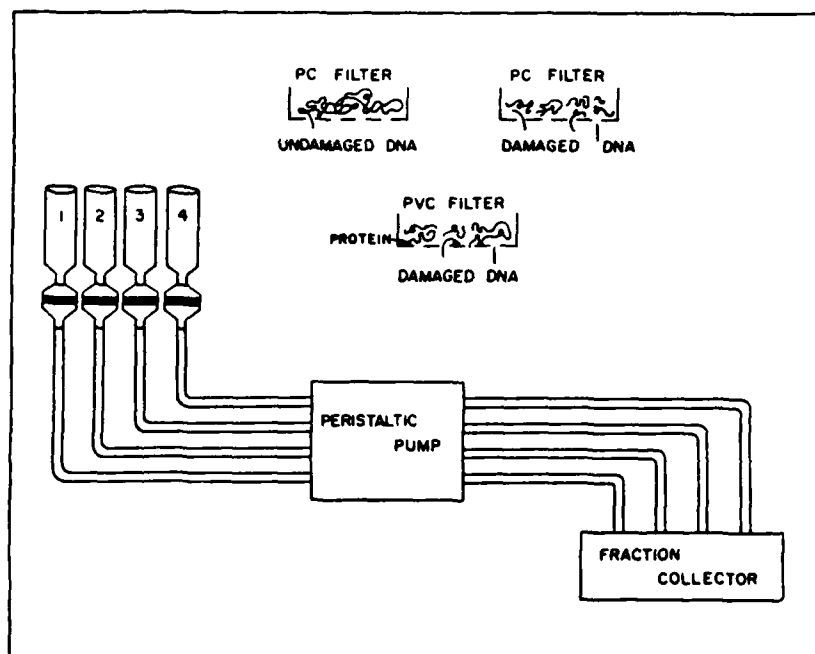


Figure 4. Schematic diagram of the alkaline elution system.

### Procedures

Exponentially growing CHO cells were labeled with  $^3\text{H}$  thymidine at a concentration of 0.05  $\mu\text{Ci/ml}$  for 24 h before analysis for DNA damage and

repair. After irradiation, CHO cells were layered on a 2  $\mu$ m PC filter and rinsed with ice-cold PBS solution and the air bubbles were removed from the filter holders. The cells were then lysed with a sodium dodecyl sulfate-ethylenediaminetetraacetate (SDS-EDTA) solution. After lysing, the cells were rinsed with 0.02 M EDTA, pH 10 (wash solution). Following this, a tetrapropyl ammonium hydroxide EDTA (pH 12.1) solution was added and the tubing was connected to an 8-channel peristaltic pump. The filter holder was covered with black paper to prevent light from producing DNA strand breaks during lysis and elution. Elution was carried out by collecting 90-min fractions at a pump speed of 0.03-0.05 ml/min for periods of 15-24 h. The data from liquid scintillation counts were analyzed to determine the fraction of DNA remaining on the filter.

## Premature Chromosome Condensation

### Principles

In 1970, Johnson and Rao (11) discovered that if a mitotic cell is fused with an interphase cell using Sendai virus, the interphase chromatin is induced to condense into discrete chromosome units, the prematurely condensed chromosomes (PCC). In this method, cells from G<sub>1</sub> phase give rise to PCC with one chromatid per chromosome, whereas G<sub>2</sub> PCC exhibit two chromatids per chromosome. The S phase PCC appear pulverized, yet both single (prereplicative) and double segments (postreplicative) can be recognized.

The PCC method has been shown to be a powerful cytogenetic tool and has been successfully used in problems involving cell cycle analysis, diagnosis of human leukemia, and evaluation of risk assessment from radiation and chemical exposure. As little as 5-rad radiation damage to human lymphocyte chromosome can be detected by the PCC method (12). In addition, when the PCC assay is used in combination with the alkaline elution technique, both DNA damage and chromosome damage can be viewed under the same experimental conditions at the same time.

### Procedures

The PCC procedures used were adapted from Pantelias's method (13) in which the Sendai virus was replaced by polyethylene glycol (PEG) as a fusogen to fuse mitotic and interphase cells.

Exponentially growing CHO cells were routinely maintained in F-10 medium supplemented with 10% fetal calf serum. Mitotic CHO cells were harvested by selective detachment following 4-h colcemide (0.2  $\mu$ g/ml) treatment. Cell fusion was performed in a glass test tube with a mixture of 3 parts interphase cells and 1 part mitotic cells. The cell mixture was first centrifuged at 200 x g for 5 min and the supernatant was discarded. A 0.25-ml volume of 55% PEG was added all at once to the cell pellet and held for 1-min exposure. The cell pellet was then resuspended in Hank's balanced salt solution and centrifuged to remove PEG solution. Finally, the cell pellet was resuspended in 0.5-ml chromosome medium 1A (Gibco) and 0.05-ml colcemide before incubating at 37 °C for 1 hr to complete the fusion process. For chromosome and slide preparation of fused cells, a hypotonic KCl solution (0.075 M) was added for 10 min at room temperature, and the cells were fixed

in methanol:acetic acid (3:1). The fixed cells were then dropped on precleaned wet slides, air dried, and stained with 3% Giemsa for PCC analysis. A typical PCC preparation from untreated G<sub>1</sub> CHO cells is shown in Figure 5.

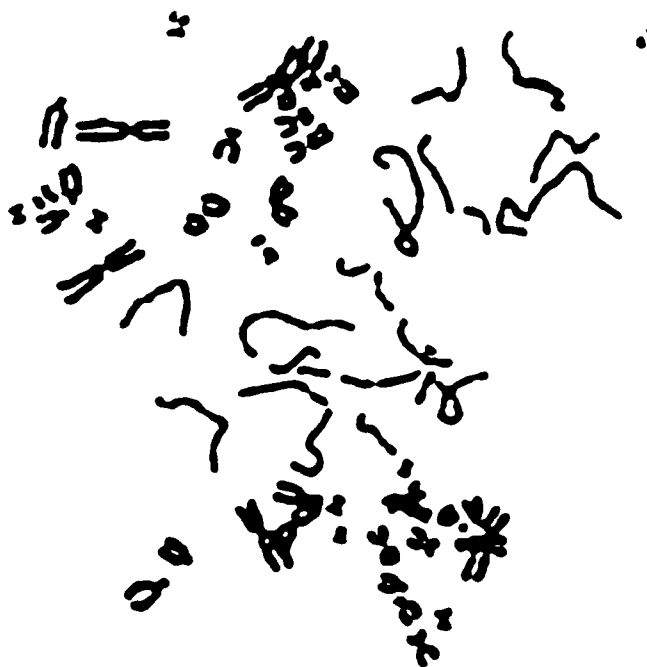


Figure 5. Premature chromosome condensation obtained from a PEG fused CHO mitotic and interphase cell. The heavy strands represent the chromosome from mitotic CHO cells and the light strands are the chromatids from interphase CHO cells. Total of 20 pairs of chromosomes are in the CHO cells.

#### Analysis of Radiation Effects on Peripheral Blood Cells

##### Immunofluorescence: Cell Preparation

Peripheral blood was obtained from the tail vein by making a small incision in the ventral side of the tail. Approximately 1 ml of blood/mouse was collected into a tube containing 100 units of heparin to prevent clotting.

The red blood cells (RBC) were lysed by adding 50 ml of NH<sub>4</sub>Cl in TRIS base, and incubating at 4 °C for 10 min. The cells were pelleted by centrifuging for 20 min at 2000 rpm and were washed once with 50 ml of PBS containing 1.0% bovine serum albumin (BSA) and 0.1% sodium azide. The cells were then counted and resuspended at  $2 \times 10^7$  cells/ml in the PBS-BSA-azide solution.

## Immunofluorescence Staining

Round-bottom, 96-well microtiter plates were used for the staining procedure. The PBS-BSA-azide solution was used throughout for all dilutions and washes. In each well was placed 0.05 ml of cells ( $2 \times 10^7$  cells/ml), and 0.05 l of diluted antibody (20  $\mu$ g/ml) was added.

The plates were incubated on ice for 15 min, and then centrifuged for 10 min at 1000 rpm. The supernatant was aspirated and 0.1 ml of wash solution added and the plates recentrifuged. The cells were then resuspended to 1 ml ( $1 \times 10^6$  cells/ml) for flow cytometric analysis. Propidium iodide (0.05 mg/ml) was added just prior to analysis to stain nonviable cells.

A flowchart for these procedures is presented in Figure 6.

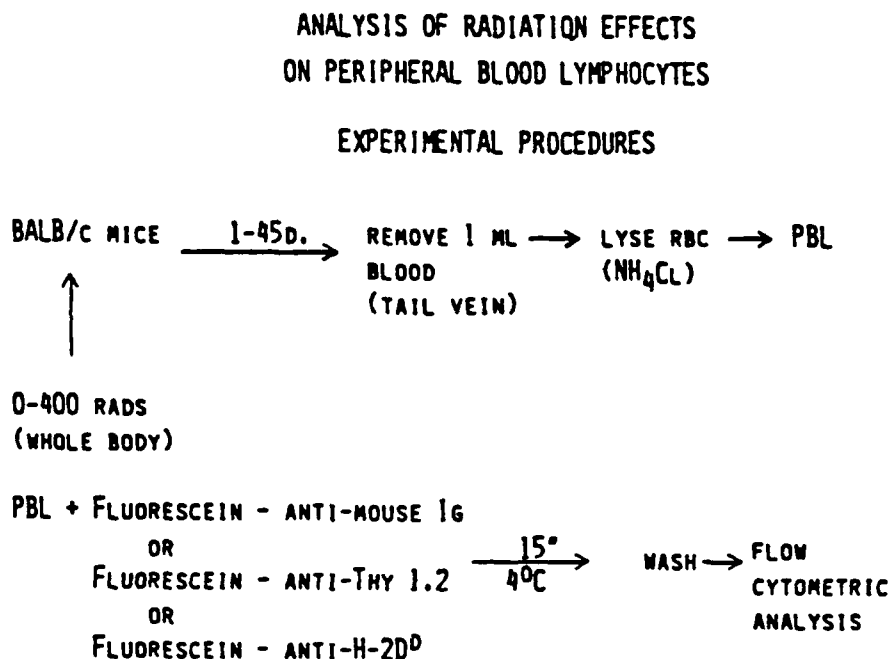


Figure 6. Flowchart of experimental procedures for analysis of radiation effects on peripheral blood lymphocytes.

## Assays of Lymphocyte Function: Mitogenic Response Assays

Mice were sacrificed by cervical dislocation. The spleens were removed and single cell suspensions prepared by gently rubbing the organ between two glass slides. The spleen cells were suspended in 1 ml of balanced salt solution (BSS) and centrifuged at 1000 rpm for 10 min. The cells were washed once by resuspending in BSS and recentrifugated. The cells were then resuspended at  $3 \times 10^6$  cells/ml in Roswell Park Memorial Institute (RPMI) 1640 media containing 10% fetal bovine serum (FBS). In each well was placed

0.10 ml of cells ( $3 \times 10^5$ ) of 96-well flat-bottomed microtiter plates. Mitogens were added to each well in 0.1-ml volume at the following concentrations: Concanavalin A (Con A), 5  $\mu\text{g/ml}$ ; and Lipopolysaccharide, 30  $\mu\text{g/ml}$  (final concentrations in wells). The cells were incubated at 37 °C for 72 h and then pulsed with  $^3\text{H}$ -thymidine (1  $\mu\text{Ci/well}$ ) for 6 h. The cells were then collected onto filter paper and placed in vials; the radioactivity was counted using a liquid scintillation counter.

### **Irradiation**

Ionizing radiation was delivered from a  $^{137}\text{Cs}$  source (J. L. Shepherd Model 81-14). Dose rates up to 562 rads/min were available. This high dose rate is used for irradiation of mice since the time required is small, resulting in minimal stress to the animals. Mammalian cell cultures are generally irradiated with dose rates between 100 and 200 rads/min.

### **Animals**

After preliminary studies confirmed the feasibility of the use of mice, we decided to use male mice of the BALB/cBy strain. These mice are readily available from a reputable supplier and are genetically compatible with many of the other types of experiments being conducted in this laboratory. We have been able to obtain sufficient blood from the tail vein to perform these studies.

## **RESULTS**

Whole-body irradiation of mice produced a decrease in total white blood cell count which was most marked at day 4 post irradiation (Fig. 7). Significant effects were observed after 100 rads.

Table 1 indicates the effects on the numbers of the different major subpopulations of white blood cells at different times after 100 and 400 rads. The most marked response is in the lymphocyte compartment (e.g., the percentage of lymphocytes decreased from 50-60% in nonirradiated controls to 24% after 100 rads on day 2). After 400 rads, the percentage of lymphocytes was still decreased (16%) at days 4 and 6, but returned to normal by day 13 post irradiation.

TABLE 1. DIFFERENTIAL CELL COUNTS ON PERIPHERAL BLOOD  
SUBPOPULATIONS FOLLOWING IRRADIATION

| Treatment<br>(rads) | Days<br>post irradiation | Percentage of total cells |             |              |
|---------------------|--------------------------|---------------------------|-------------|--------------|
|                     |                          | Lymphocytes               | Macrophages | Granulocytes |
| 0                   | 2                        | 52.8                      | 12.0        | 35.2         |
|                     | 4                        | 63.3                      | 13.3        | 24.1         |
|                     | 6                        | 60.2                      | 14.6        | 25.2         |
|                     | 13                       | 66.6                      | 12.4        | 21.0         |
| 100                 | 2                        | 24.1                      | 10.1        | 65.6         |
|                     | 4                        | 47.8                      | 24.1        | 28.1         |
|                     | 6                        | 56.2                      | 13.8        | 30.0         |
|                     | 13                       | 60.8                      | 11.5        | 27.8         |
| 400                 | 2                        | nd                        |             |              |
|                     | 4                        | 16.5                      | 29.1        | 54.4         |
|                     | 6                        | 16.3                      | 18.5        | 65.5         |
|                     | 13                       | 63.0                      | 15.2        | 21.8         |

Mice (3 mice/group/time point) were irradiated (0, 100, 400 rads) and the PBL removed at various days later. Cytocentrifuge slides were prepared, stained with a modified Wright's Giemsa stain, and differential counts done, counting 500 cells/slide.

# EFFECT OF RADIATION ON THE NUMBER OF WHITE BLOOD CELLS

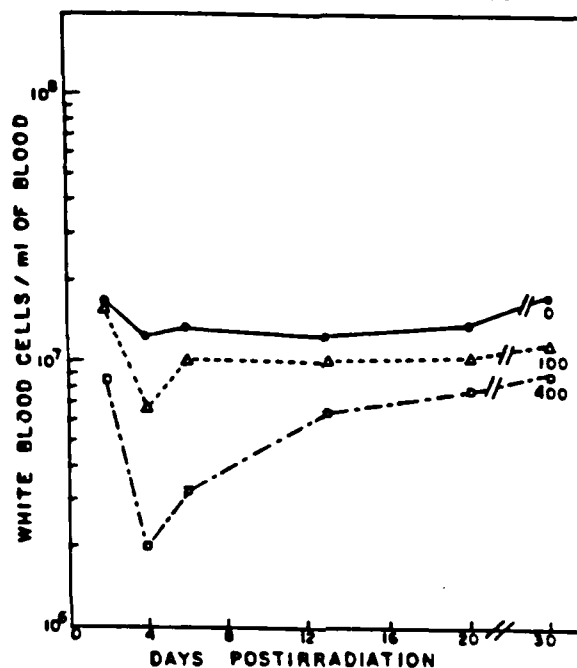


Figure 7. Kinetics of the radiation dose response of the number of white blood cells/ml of blood present after 0-rad (●), 100-rad (Δ), or 400-rad (□) whole-body irradiation.

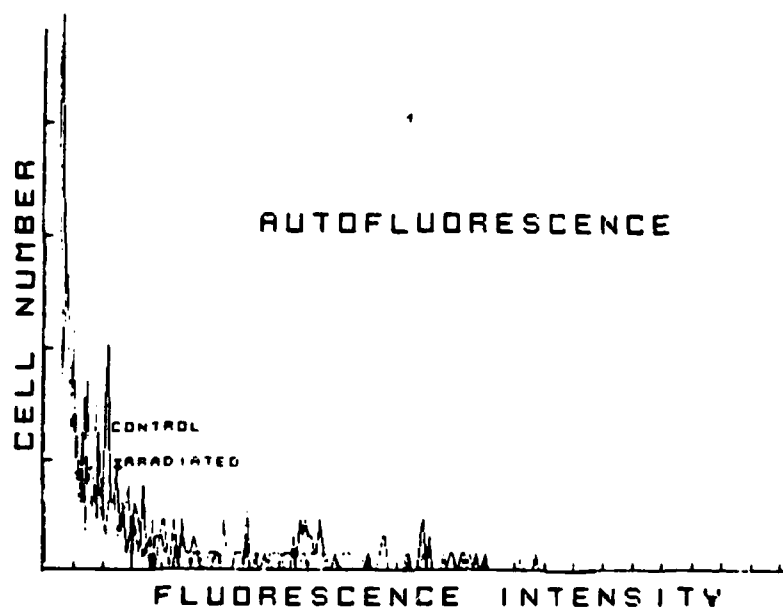


Figure 8. Two-dimensional flow cytometry histogram showing the autofluorescence of unstained peripheral blood lymphocytes from control mice and irradiated (400 rads) mice 7 days post irradiation.



To examine the radiation sensitivity of subpopulations within the white blood cells, and especially the lymphocyte compartment, we have used flow cytometry and immunofluorescence techniques. Figure 8 shows the normal autofluorescence of cells on a 2-dimensional histogram of cell number vs fluorescence intensity. A total of 20,000 cells were analyzed. It can be seen that there was no difference between the autofluorescence obtained for white blood cells from control compared with those from irradiated (400 rads) mice when analyzed on day 7 (results at other times post irradiation were similar).

By using an antibody to H2 class 1 antigens, it is possible to measure the radiation-induced decrease in the white blood cells (lymphocytes, macrophages, and granulocytes) using flow cytometry fluorescence analysis (Fig. 9). The fluorescence distribution curve indicates at least two main populations within the white cell compartment. Irradiation appears to affect the population with the greatest fluorescence intensity.

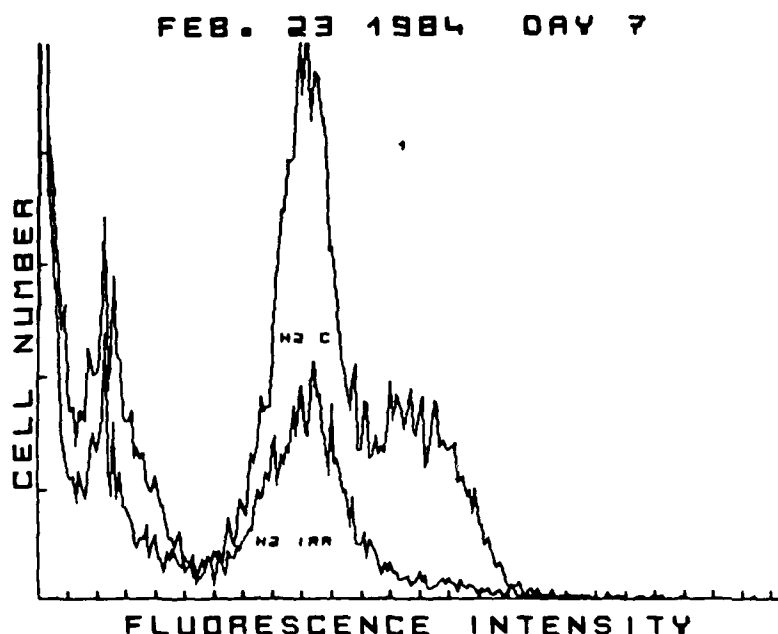


Figure 9. Two-dimensional flow cytometry histogram showing the differences in intensity of H-2D<sup>d</sup> surface fluorescence staining of control cells (H-2C) and PBL from mice receiving 400-rad whole-body irradiation 7 days previously.

Figure 10 shows the decrease in the Thy 1 lymphocyte compartment induced by irradiation. Positive cells are indicated by the peak to the right side of the fluorescence histogram. This lymphocyte subpopulation was relatively sensitive to irradiation (400 rads, day 7 postirradiation).

The B-lymphocyte population, as measured by the binding of an antibody-to-surface immunoglobulin (Ig), was even more sensitive (Fig. 11). A dose

FEB. 23 1984 DAY 7

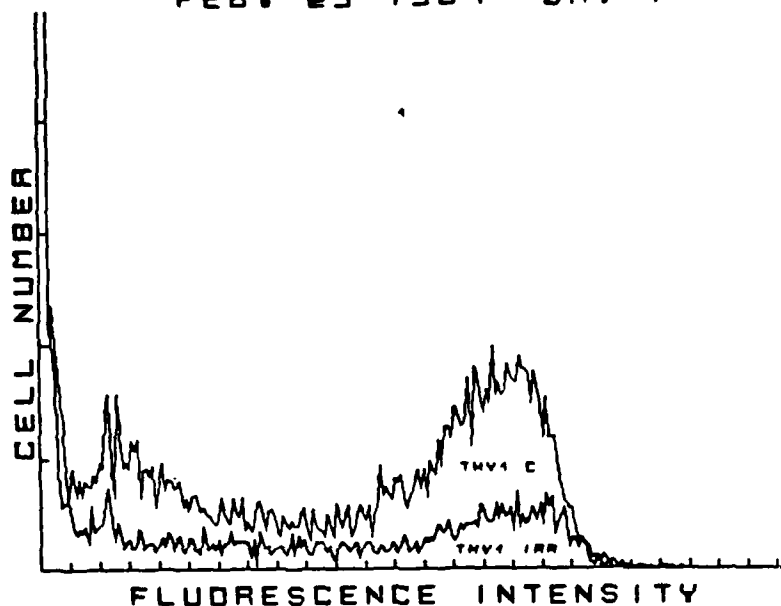


Figure 10. Two-dimensional flow cytometry histograms showing a marked decrease in cells positive for the T-cell marker Thy-1 in mice receiving 400-rad irradiation (Thy-1 Irr) as compared to control mice (Thy-1 C).

FEB. 23 1984 DAY 7

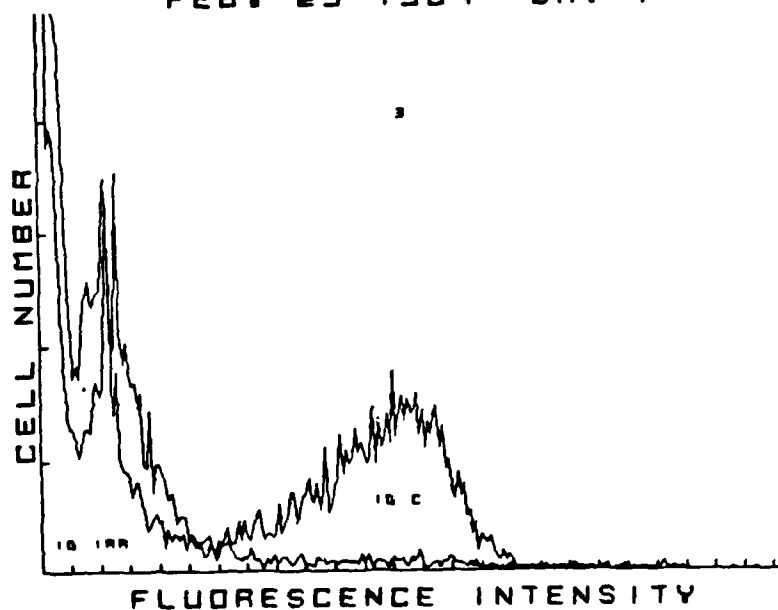


Figure 11. Two-dimensional flow cytometry histogram showing the virtual elimination of surface Ig<sup>+</sup> cells (B-lymphocytes) of the PBL from mice receiving 400-rad irradiation.

of 400 rads almost completely eliminated the binding by this antibody at day 7.

These data and results for another dose (100 rads) and at other post irradiation times are summarized quantitatively in Table 2. The maximum effect appears to occur at about day 4 post irradiation. The B-lymphocytes are more sensitive than the Thy 1 subclass. For example, on day 4 after 100 rads, the ratio of irradiated control Thy 1 cells was about 0.6, whereas this ratio for B cells was about 0.3.

TABLE 2. FLOW CYTOMETRIC ANALYSIS OF THE EFFECT OF RADIATION ON PERIPHERAL BLOOD SUBPOPULATION

| Treatment<br>(rads) | Days<br>post irradiation | Number of cells ( $\times 10^{-6}$ )/ml Blood |                    |                 |
|---------------------|--------------------------|---|--------------------|-----------------|
|                     |                          | H-2 <sup>d</sup> +                            | Thy 1 <sup>+</sup> | Ig <sup>+</sup> |
| 0                   | 2                        | 7.18  | 2.32               | 5.76            |
|                     | 4                        | 5.49  | 2.56               | 4.58            |
|                     | 6                        | 7.72  | 3.50               | 6.62            |
|                     | 13                       | 5.87  | 1.69               | 3.28            |
| 100                 | 2                        | 6.27  | 1.50               | 5.23            |
|                     | 4                        | 2.66  | 0.85               | 1.90            |
|                     | 6                        | 5.70  | 2.13               | 4.50            |
|                     | 13                       | 5.14  | 0.66               | 4.35            |
| 400                 | 2                        | 3.69  | 0.95               | 2.43            |
|                     | 4                        | 0.83  | 0.19               | 0.57            |
|                     | 6                        | 1.82  | 0.31               | 1.51            |
|                     | 13                       | 3.57  | 0.57               | 3.16            |

Mice were irradiated as detailed in the text. On subsequent days 3 mice/group were sacrificed, bled, and PBL obtained and pooled. The PBL were stained with fluorescein-conjugated antibodies specific for H-2<sup>d</sup>, Thy 1, or surface Ig. These cells (20,000/sample) were analyzed on the flow cytometer and the percentage of positively stained cells as compared to unstained controls was obtained by analysis of the histograms using the Terak LSI-11/23 computer.

In addition to the evaluation of numbers of the white blood cell and lymphocyte compartments, the functional capacity of T- and B-lymphocytes was measured at different times after irradiation. The functional measure is the ability of the cells to proliferate in response to nonspecific mitogens, Con A for T cells, and lipopolysaccharide (LPS) for B cells. Significant changes were produced by doses of 100 and 200 rads at different times up to 5 days post irradiation in vivo (Table 3). The greatest effect was observed with B cells at day 3 following irradiation; there was a decrease in the stimulation index of a factor of about 7 ( $28 \pm 9$  for control vs  $4 \pm 3$  after irradiation). By comparison, the T cells which were responding to Con A increased relative to controls at different times after irradiation. This was probably due mainly to a decrease of numbers of B cells, as indicated by the flow cytometry-antibody data, so that the relative proportion of T cells in the population has increased. After 100 rads the response of both T- and B-lymphocytes has returned to near normal by days 4 to 5 post irradiation. However, both T- and B-lymphocytes are still decreased in functional capacity at this time after 200 rads.

TABLE 3. EFFECT OF RADIATION ON THE FUNCTION OF PERIPHERAL BLOOD LYMPHOCYTES

| Treatment <sup>1</sup><br>(rads) | Mitogen | Days post irradiation          |              |              |              |
|----------------------------------|---------|--------------------------------|--------------|--------------|--------------|
|                                  |         | 2                              | 3            | 4            | 5            |
|                                  |         | Stimulation index <sup>2</sup> |              |              |              |
| None                             | Con A   | 269 $\pm$ 124                  | 149 $\pm$ 6  | 118 $\pm$ 5  | 94 $\pm$ 35  |
| 100                              | Con A   | 420 $\pm$ 58                   | 176 $\pm$ 67 | 171 $\pm$ 40 | 139 $\pm$ 38 |
| 200                              | Con A   | 131 $\pm$ 47                   | 257 $\pm$ 36 | 229 $\pm$ 22 | 186 $\pm$ 33 |
| None                             | LPS     | 52 $\pm$ 10                    | 28 $\pm$ 9   | 45 $\pm$ 5   | 29 $\pm$ 8   |
| 100                              | LPS     | 49 $\pm$ 20                    | 18 $\pm$ 7   | 45 $\pm$ 12  | 21 $\pm$ 3   |
| 200                              | LPS     | 22 $\pm$ 15                    | 4 $\pm$ 3    | 19 $\pm$ 2   | 18 $\pm$ 4   |

<sup>1</sup> Mice were given whole-body irradiation and then sacrificed at days 2-5 post treatment. Spleen cells from individual mice were cultured  $\pm$  mitogen for 72 h followed by a 6-h pulse of <sup>3</sup>H thymidine.

$$\text{Stimulation index} = \frac{\text{CPM for cultures + mitogen}}{\text{CPM for cultures - mitogen}}$$

Using the centrifugal elutriation and alkaline elution assay, we have determined the formation and rejoining of DNA single-strand breaks and cross-links from synchronized CHO cells. A long collection elutriation method was used to separate asynchronous CHO cells into fractions of homogeneous sized subpopulations (Fig. 12). Fraction I, II, and III represent the size distribution of cells at mid  $G_1$ , mid-S, and mid  $G_2+M$  phases of the cell cycle. The DNA histograms of these fractions (Fig. 13) show a high degree of synchrony in  $G_1$ , S, and  $G_2+M$  cells. Computer analysis of the DNA histogram indicates that approximately 95%  $G_1$  cells, 80% S cells, and 80%  $G_2+M$  cells are found in fraction I, II, and III respectively.

After irradiation with 0-800-rad Cs-137 gamma ray, the formation of DNA single-strand breaks was measured with the alkaline elution assay. The profiles of alkaline elution patterns are shown in Figure 14. The initial slopes of alkaline elution profiles measured from DNA single-strand breaks are found to be first order with respect to both elution time and gamma-ray doses (Fig. 14). The rejoining of DNA single-strand breaks following a single 1000 rad gamma ray shows a progressive decrease in the elution slope as a function of repair time (Fig. 15). A linear relationship between the elution rate ( $h^{-1}$ ) and the radiation dose was established for CHO cells at different stages of the cell cycle (Fig. 16). Using this approach, radiation damage as low as 25-50 rads can be detected.

Although there is no significant difference in the formation of DNA single-strand breaks, the repair rates measured from cells at different phases of the cell cycle are different (Fig. 17). When the repair half-times are determined from fast repair process (steep slope) and slow repair process (shallow slope),  $G_2+M$  cells show a significant slower repair rate of DNA single-strand breaks than S and  $G_1$  cells. The halftimes for the fast and slow repair process in  $G_1$  and S cells are 4 min and 70 min respectively. In  $G_2+M$  cells, they become 8 min and 100 min. Since S phase cells in CHO cultures are most resistant to radiation, the DNA repair study may demonstrate a positive correlation between DNA repair capacity and radiation sensitivity in mammalian cells. Similar results were also obtained in the repair of DNA cross-links after ionizing radiation (Fig. 18). The removal of DNA cross-links as indicated by the decrease of cross-link factors (Fig. 18) is more rapid in S phase cells than  $G_1$  and  $G_2+M$  cells.

In order to relate DNA damage to chromosome damage, studies of chromosome breaks as revealed by the PCC were performed in CHO cells in the dose range of 0-500-rad Cs-137 gamma ray. Figure 19 shows the microscopic photograph of PCC measured at 100, 300, and 500 rads. Figure 20 shows the quantitative relationship between radiation dose and chromosome damage indicating significant detection of damage at 50 rads.

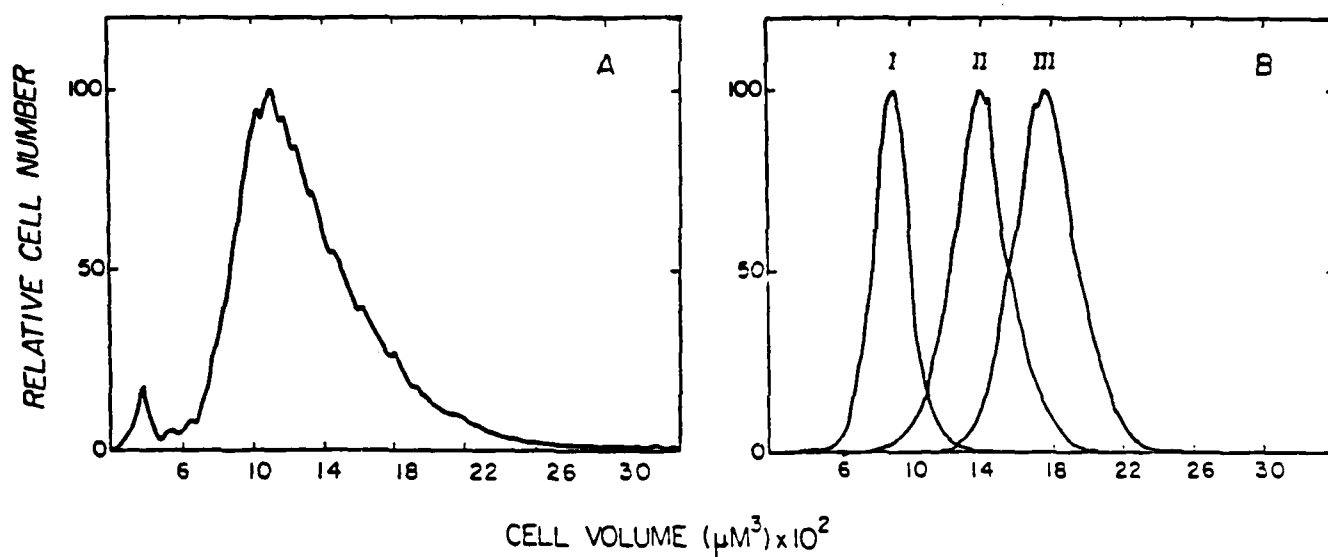


Figure 12. Cell volume distribution of unseparated (A) and elutriated (B) CHO cells measured by Coulter channelyzer.

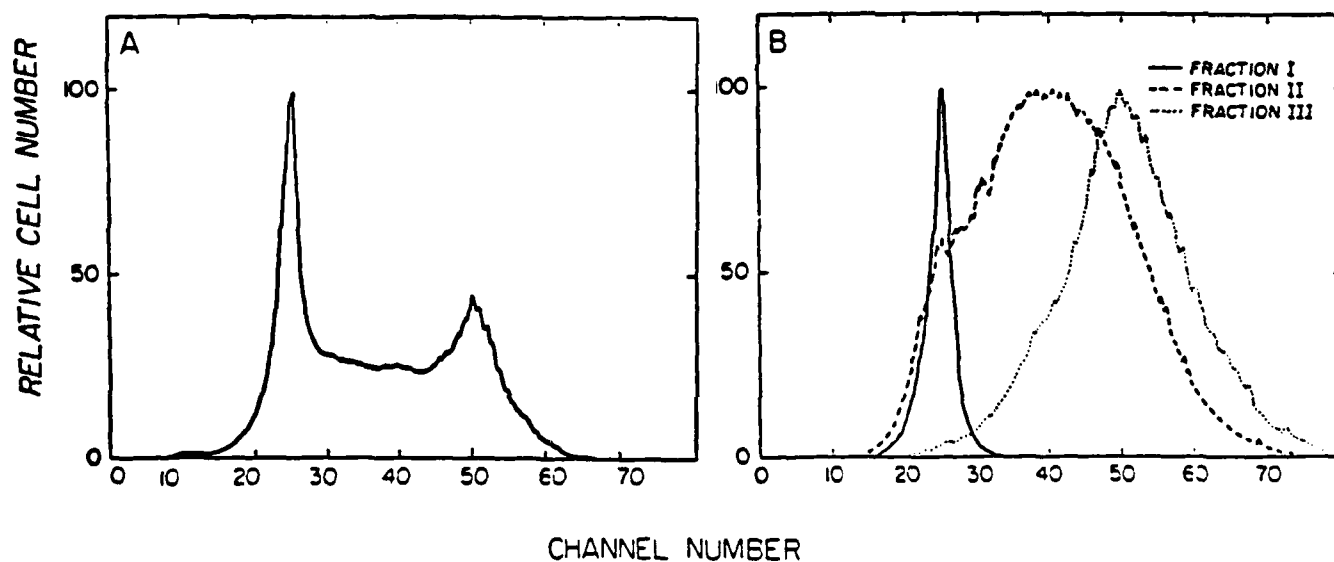


Figure 13. DNA histograms of asynchronous CHO cells (A) and separated  $G_1$ , S, and  $G_2+M$  cells (B).

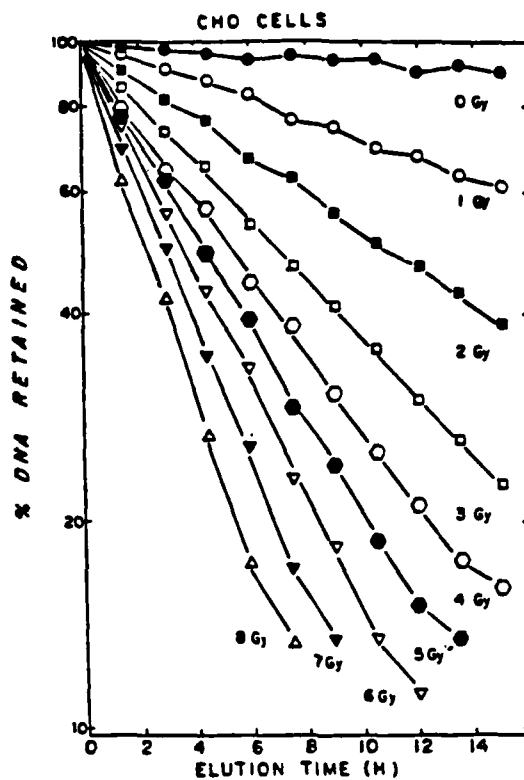


Figure 14. Alkaline elution profiles of CHO cells irradiated with 0-800-rad Cs-137 gamma rays.

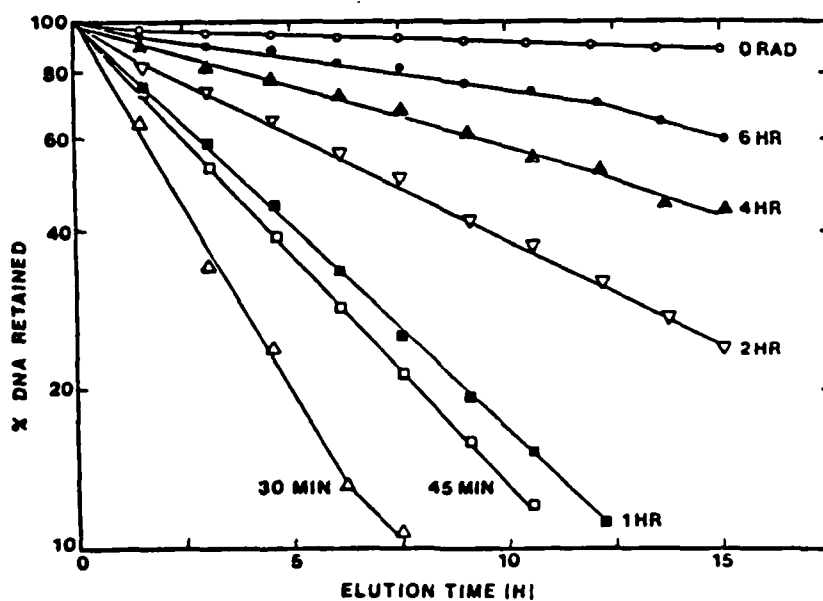


Figure 15. Alkaline elution profiles of CHO cells irradiated with a single dose of 1000 rads and incubated at 37 °C for 30 min, 45 min, 1 h, 2 h, 4 h, and 6 h.

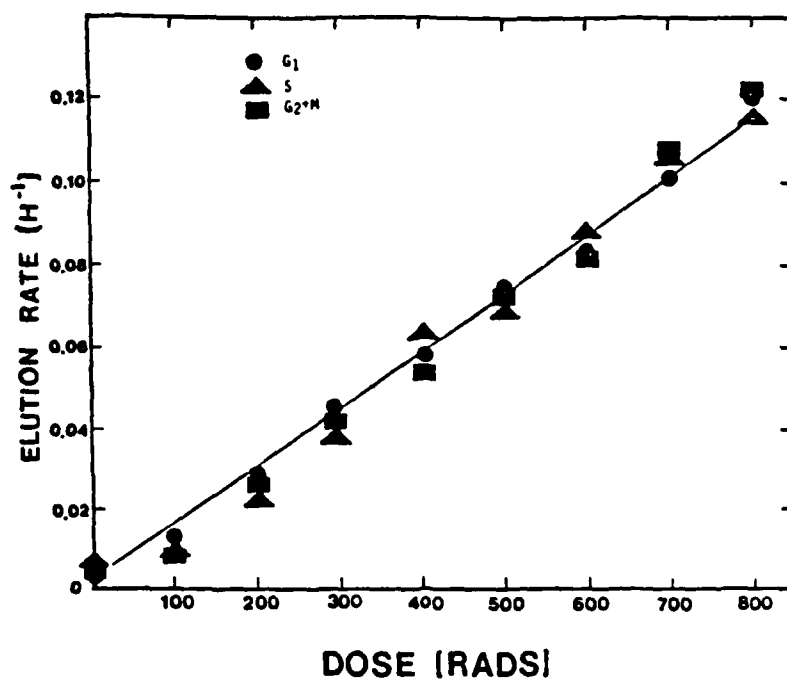


Figure 16. Formation of DNA single-strand breaks at G<sub>1</sub> , S, and G<sub>2</sub>+M phases of the cell cycle in CHO cells.

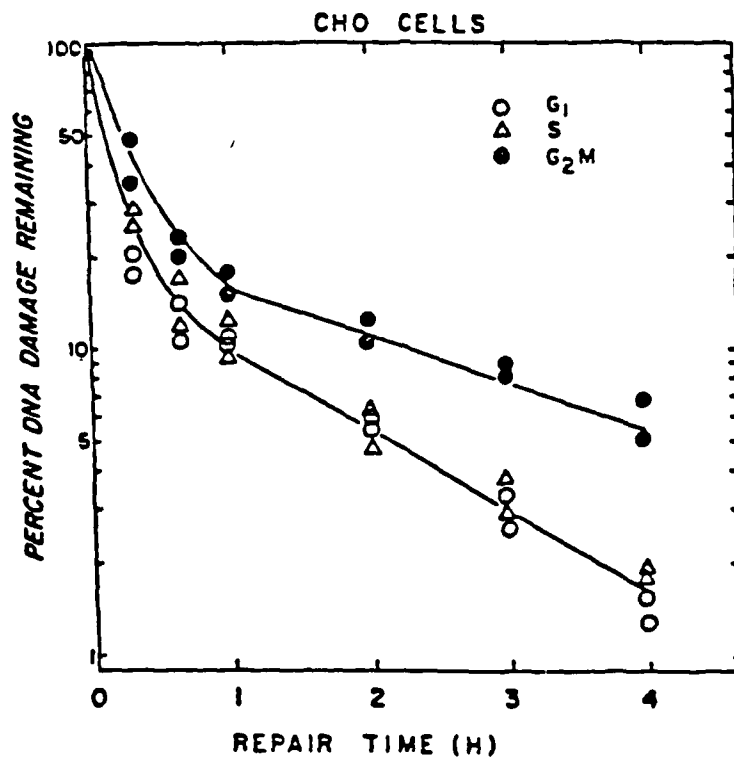


Figure 17. Repair kinetics of DNA single-strand breaks at G<sub>1</sub> , S, and G<sub>2</sub>+M phases of the cell cycle after 1000-rad Cs-137 gamma rays.



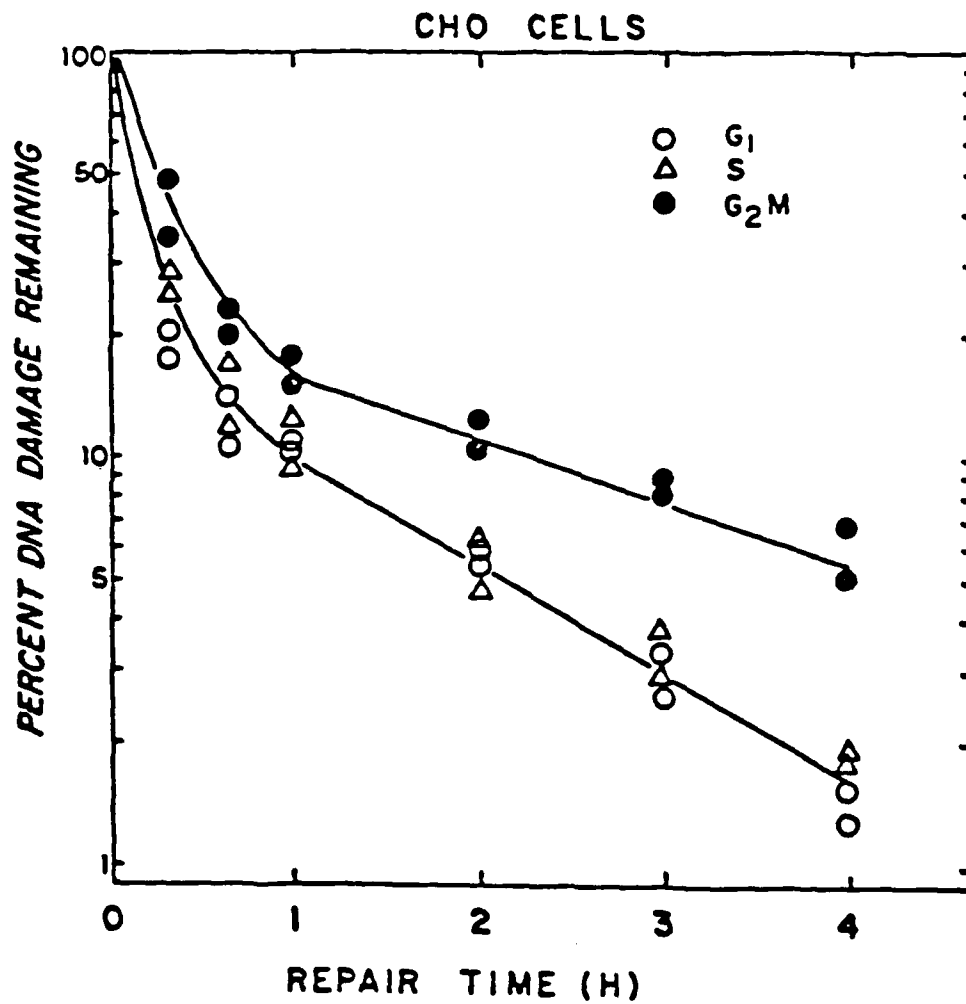
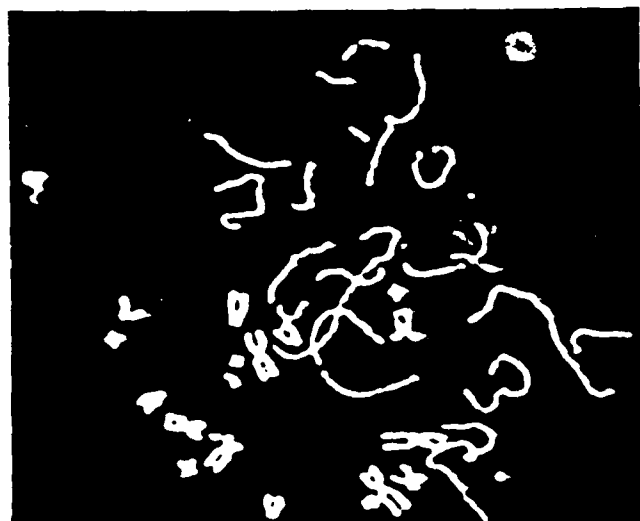


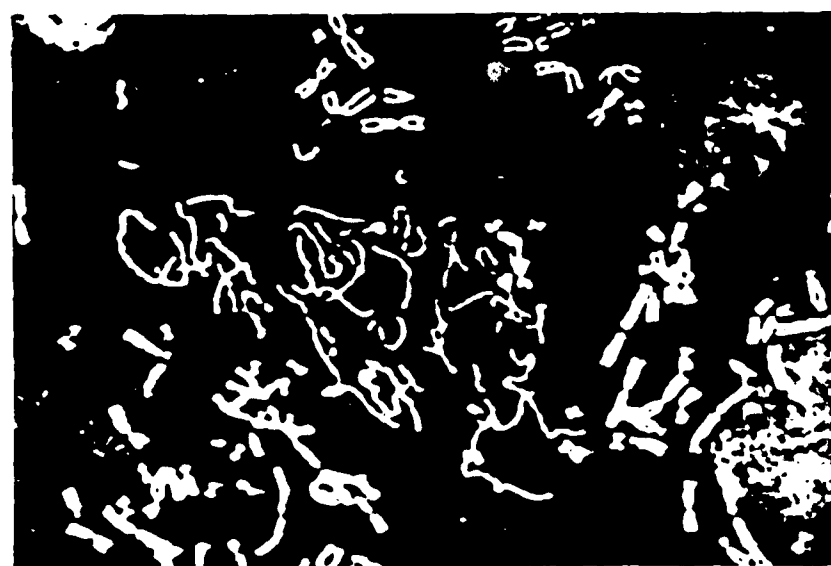
Figure 18. Repair kinetics of DNA cross-links in  $G_1$ , S, and  $G_2M$  CHO cells following 5-krad gamma rays.



A



B



C

Figure 19. Premature chromosome condensation of CHO cells irradiated with 100-rad (A), 300-rad (B), and 500-rad (C) Cs-137 gamma rays. The numbers of fragments in 100-rad, 300-rad, and 500-rad treated cells are 23, 36, and 56, respectively.

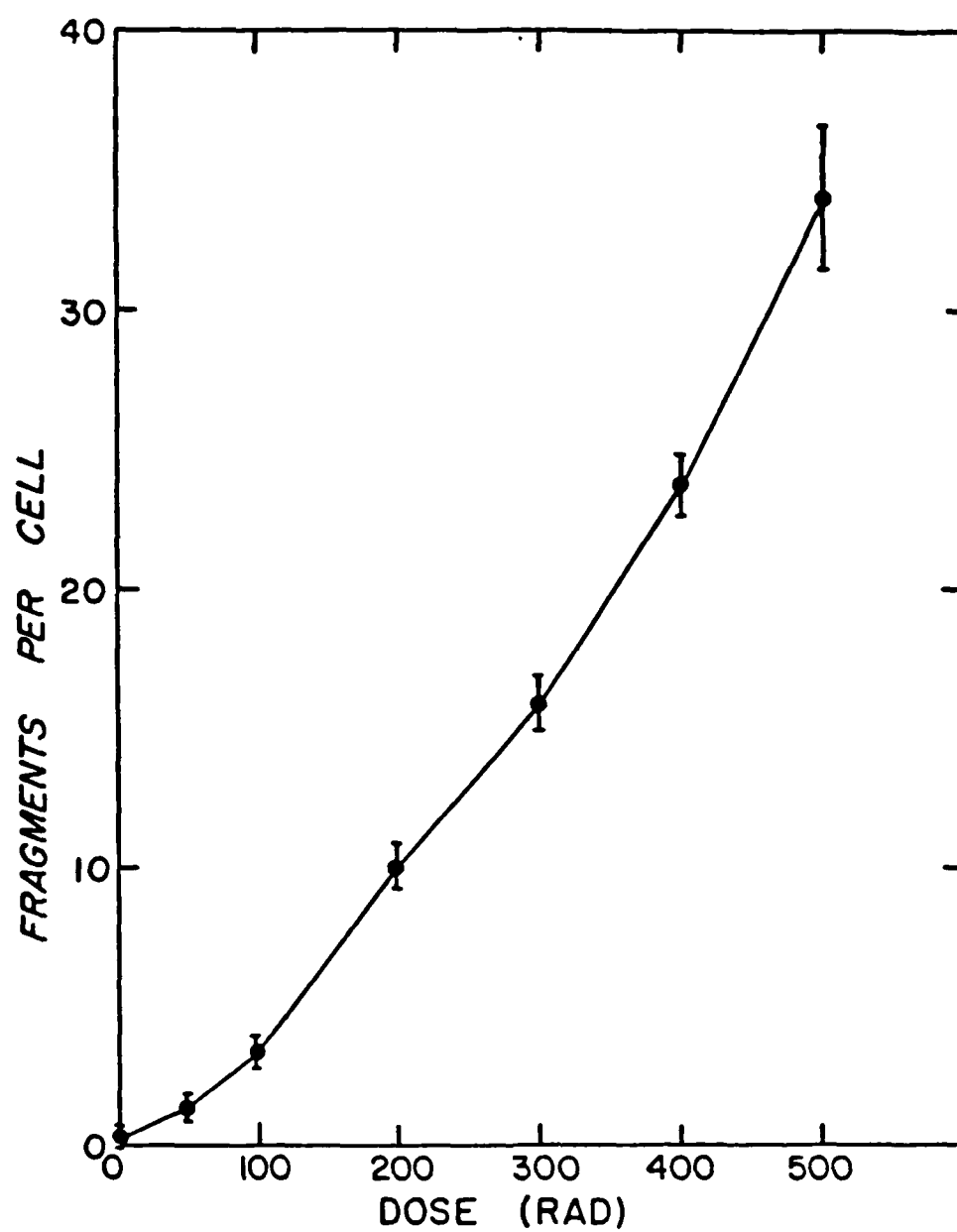


Figure 20. Relationship of radiation dose and chromosome aberrations in CHO cells irradiated with 0-500-rad Cs-137 gamma rays.

## DISCUSSION

The results demonstrate the application of several relatively new technologies to measure the radiation sensitivities of different subpopulations of cells. These technologies include centrifugal elutriation, flow cytometry, monoclonal antibodies, alkaline elution for DNA damage and repair, and premature chromosome condensation for chromosome damage. Significant differences in radiation sensitivity of subpopulations were observed, indicating the potential of this experimental approach to improve the quantitative measurement of relatively low doses of radiation. Two general areas of research were pursued: the radiation sensitivity of lymphoid cell populations of peripheral blood irradiated in vivo, and DNA/chromosome damage and repair of normal mammalian cells in culture irradiated in vitro.

It appears that the B-lymphocytes are more sensitive than the T-lymphocytes. Changes in numbers, antigen expression, and functions of cells in both these compartments were observed. Doses of 100 rads produced large effects. It appears probable that a combination of these different types of assays could provide a very sensitive index of radiation exposure for doses considerably less than 100 rads. Additional experiments are required to accurately define the dose-response relationship.

Deoxyribonucleic acid damage of CHO cells, as measured by alkaline elution was linearly related to radiation dose. This relationship was quantitatively similar for cells at different stages of the cell cycle. Radiation damage in the 25-50-rad range can be detected by this method. It was also shown that the DNA damage could be repaired. Both slow and rapid repair components were detected. Damage was repaired more rapidly by S and G<sub>1</sub> phase cells. The enhanced repair of S phase cells correlates with the increased resistance of these cells at this cell cycle phase as measured by colony formation assays (other previous studies).

Chromosome damage in the form of breaks could be measured in CHO cells using the premature chromosome condensation method. Data were obtained to demonstrate the dose response relationship for those cells which indicated a curvilinear relationship at lower doses. These cells also express a shoulder on the survival curve (colony formation assay) which appears to correlate. Additional experiments are required to establish this dose-response curve for the sensitive subpopulations of lymphocytes. It appears that doses less than 50 rads are readily detectable in CHO cells. On the other hand, lymphocytes are generally more sensitive and usually express linear radiation dose-response curves. Damage from a dose of 5 rads was recently detected for human peripheral blood lymphocytes using this method (13). Based on these data and the demonstration here of even greater radiation sensitivity of certain lymphocyte subsets, it seems possible to increase the sensitivity if isolated subpopulations are analyzed by this method.

Future research is required to determine the dose response relationships for mouse and human peripheral blood lymphocytes using these different assays, and to establish whether a combination of several different types of measurements will provide a very sensitive index useful as a radiation biodosimeter. If this can be established, the next phase of research could analyze blood specimens obtained from space crews and/or experimental animals exposed

to radiation in space to determine the sensitivity and relate the results to data obtained from physical dosimeters. Additional experiments would be required to evaluate effects of different radiations of known linear energy transfer (LET). Research conducted in parallel would be necessary to determine ways to conveniently and simply obtain enriched fractions of radiation sensitive lymphocytes and to prepare and preserve these for analyses during space flights of long duration. This research may also require test flights of certain modified equipment necessary for these assays as well as in-flight experiments.

#### REFERENCES

1. Anderson, R. E., and N. L. Warner. Ionizing radiation and the immune response. *Adv. Immunol.* 24:216-335 (1976).
2. Lindahl, P. E. Principle of a counter-streaming centrifuge for the separation of particles of different sizes. *Nature* 161:648-649 (1948).
3. Keng, P. C., C. K. N. Li, and K. T. Wheeler. Characterization of the separation properties of the Beckman Elutriator system. *Cell Biophysic* 3:41-56 (1981).
4. Bonner, W. A., H. R. Huett, R. G. Sweet, and L. A. Herzenberg. Fluorescence activated cell sorting. *Rev.Sci.Inst.* 43:404-408 (1972).
5. Shapiro, H. M. Multistation multiparameter flow cytometry: A critical review and rationale. *Cytometry* 3:227-235 (1983).
6. Horan, P. K., and L. L. Wheless. Quantitative single cell analysis and sorting. *Science* 198:149-157 (1977).
7. Kohler, G., and C. Milstein. Continuous culture of fused cells secreting antibody of predefined specificity. *Nature* 256:495-497 (1975).
8. Loken, M. R., and A. M. Stall. Flow cytometry as an analytical and preparative tool in immunology. *J.Immunol.Meth.* 50:R85-R112 (1982).
9. Dean, P. N., and J. H. Jett. Mathematical analysis of DNA distributions from flow microfluorometry. *J.Cell Biol* 60:523-527 (1974).
10. Kohn, K. W., and R. A. Grimek-Ewig. Alkaline elution analysis, a new approach to the study of DNA single-strand interruptions in cells. *Cancer Res.* 33:1849-1853 (1973).
11. Johnson, R. T., and P. N. Rao. Mammalian cell fusion: induction of premature chromosome condensation in interphase nuclei. *Nature* 226:717-722 (1970).
12. Pantelias, G. E., and H. D. Maillie. The use of peripheral blood mononuclear cell prematurely condensed chromosomes for biological dosimetry. *Radiat.Res.* 99:140-150 (1984).
13. Pantelias, G. E., and H. D. Maillie. A simple method for premature chromosome condensation induction in primary human and rodent cells using polyethylene glycol. *Somatic Cell Genetics* 9:533-547 (1983).

END  
DTIC

7-86